Efficient synthesis of ordered organo-layered double hydroxides†

H. Christopher Greenwell,*[a] William Jones,[b] Sarah L. Rugen-Hankey,[c] Peter J. Holliman[c] and Richard L. Thompson[a]

Received 10th August 2009, Accepted 9th February 2010
First published as an Advance Article on the web 22nd February 2010
DOI: 10.1039/b916301h

Layered double hydroxides (LDHs) intercalated with terephthalate anions represent one of the most studied organo-LDH systems. We have prepared MgAl terephthalate-LDHs using an efficient hydrothermal approach from the respective metal hydroxide precursors. In contrast to terephthalate LDHs prepared by other methods, and as a result of the absence of competing anions, a large excess of terephthalate acid was not required, thereby allowing for an environmentally attractive synthetic route. The LDHs were prepared from starting reactant Mg/Al ratios of 2, 3, 4 and 5 and were found to exhibit unusually high degrees of order as evidenced from X-ray diffraction studies, especially at the Mg/Al ratio of 2. Further analysis of the X-ray diffraction data showed that, as in previous studies, three distinct interlayer arrangements could be identified. Scanning electron microscopy was used to compare and contrast the morphology of crystals formed with those prepared by other methods of LDH synthesis and confirms the high degree of structural integrity achieved by the synthetic method.

1. Introduction

Layered double hydroxides (LDHs), also known as anionic clays or hydrotalcite-like compounds, are members of the layered host class of compounds. Other members of this class of materials include graphite, cationic clays, transition metal dichalcogenides and metal phosphates. These compounds all exhibit the property of intercalation—the incorporation of guest species between the sheets of a layered host. Owing to this property, these materials have current uses and further potential applications as adsorbents,[1] biofuel and other catalysts,[2] constrained nanoscale reaction vessels,[3] pharmaceuticals,[4] and as fillers in nanocomposite materials.[5] The synthesis, characterisation and application of LDHs in general have been recently reviewed.[6,7]

Fig. 1 illustrates the layered structure of an LDH. Layers consisting of M^{2+} and M^{3+} ions are octahedrally co-ordinated by hydroxyl anions and the resulting octahedra sharing edges to form layers. The structure is analogous to that of brucite ($Mg(OH)_2$) except some of the M^{2+} have undergone isomorphous replacement by M^{3+} ions, resulting in an overall positive charge. This charge is balanced by the presence of anions, depicted as $A^{n}-$ in Fig. 1, which, together with water, occupy the space between the layers. LDH materials can be considered across a range of length-scales: (i) as exfoliated single sheets where the variables are aspect ratio and metal ion composition;[8] (ii) as crystals where sheets stack together with variably stacking sequence giving rise to polytypism;[9] (iii) as macroscopic structures where LDHs are formed around organic or inorganic templates.[10]

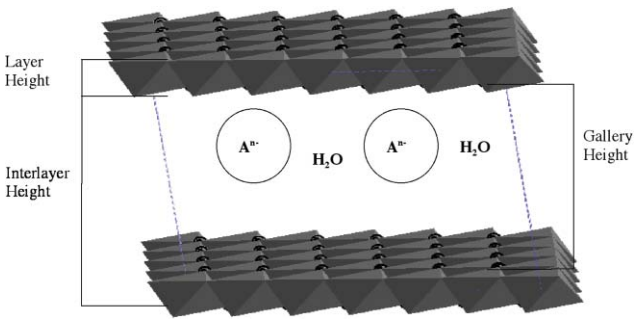

Fig. 1 Schematic to show the general structure of a layered double hydroxide. The grey octahedra represent the LDH sheets and $A^{n}-$ represent charge balancing anions.

Terephthalate (TA) LDHs have been used as precursors for the preparation of polyoxometallate pillared anionic clays,[11–14] with the TA anion facilitating the insertion of bulkier anions within the gallery region. In a similar manner TA LDH precursors have been applied to the synthesis of nanocomposites containing polyaniline.[15] The relatively rigid nature of the TA anion has enabled studies on the dynamics of interlayer anions, both by spectroscopic,[16] and computational,[17] studies. In addition to LDHs, the TA anion has been incorporated into other layered inorganic/organic hybrids such as metal hydroxides.[18,19] As such, the TA LDH system provides a good reference for testing new organo-LDH preparative techniques.

Drezdon carried out the earliest synthesis of a TA LDH in 1988,[11] and since then, the TA anion has been intercalated into

[a]*Department of Chemistry, Durham University, South Road, Durham, UK DH1 3LE. E-mail: chris.greenwell@durham.ac.uk; Fax: +44 (0)1913 844737; Tel: +44 (0)1913 342105*
[b]*Department of Chemistry, University of Cambridge, Lensfield Road, Cambridge, UK CB2 1EW*
[c]*School of Chemistry, Bangor University, Bangor, Gwynedd, UK LL57 2UW*

† Electronic supplementary information (ESI) available: (1) synthetic methods for preparation of the comparative samples used in the FEGSEM analysis; (2) FTIR spectra and discussion; (3) schematic of interlayer arrangements. See DOI: 10.1039/b916301h

a wide variety of M^{+}/M^{3+}, M^{2+}/M^{3+} and $M^{2+}/M^{2+}/M^{3+}$ LDHs including M^{+} as Li, M^{2+} as Zn, Co, Mg, Ca and M^{3+} as Cr, Ga, or Al. Though Drezdon used a variable pH co-precipitation method, subsequently anion exchange was used for the synthesis of TA LDHs.[20] For a general LDH synthesis method, the anion-exchange method was found to be restrictive in selectivity of the organic anion and was superseded by a development of the co-precipitation method,[21,22] and the re-hydration (reconstruction) route.[23,24] The co-precipitation method was further extended by the constant pH technique,[25] which allowed the influence of layer charge and carbonate content to be systematically examined.

The co-precipitation method using metal nitrate salts of high solubility, at variable or constant pH, has since been the main synthetic route to TA-LDHs.[6,17,26–28] Drawbacks of this method from a green chemistry perspective are: (i) to exclude nitrate intercalation a large excess, up to twenty fold, of the anion must be used; (ii) the scale of the reaction is somewhat limited; (iii) certain anions can be difficult to intercalate, mainly those with low charge-to-mass; (iv) owing to the relatively low slurry weights used, copious amounts of a highly basic waste stream are generated. In order to address some of these challenges, we, and others, have been investigating use of other methods, such a organo-metal salts and metal oxides as the M^{2+}/M^{3+} source to generate organo-LDHs which have high chemical efficiency, use concentrated slurries and near neutral pH waste streams.[29–33] Ogawa and Sugiyama also utilised ZnO and $Al(OH)_3$ to prepare ZnAl LDHs at very high slurry loadings of *ca.* 20 g product per 100 ml of reactant solution.[34] In other work, Ogawa and Asai also utilised the metal hydroxides ($Al(OH)_3$ and $Mg(OH)_2$ as used here) as the metal source,[35] under hydrothermal conditions, to overcome low anion selectivity in anion exchange/co-precipitation reactions, in the preparation of a deoxycholate intercalated LDHs. The hydroxides are an attractive source of M^{2+}/M^{3+} from a green chemistry perspective, as the reactive oxides are generated from energy intensive calcination of the hydroxides. As such, we extend our previous work in this area by examining the metal hydroxide method of preparation in the present study.

2. Experimental

The $Mg(OH)_2$ used was obtained from Aldrich in 95% purity. Gibbsite ($Al(OH)_3$) was from Huber Micral and the terephthalic acid (98% purity) was from Lancaster. All reagents were used as received.

A typical preparation is described for Mg/Al ratio (*R*) of 3.0. A 10% by weight aqueous dispersion of $Mg(OH)_2$ (5.00 g, 86.20 mM $Mg(OH)_2$ in 95 g of deionised H_2O) was prepared under atmospheric conditions. To this was added $Al(OH)_3$ (2.24 g, 28.74 mM) and terephthalic acid (14.37 mM, 2.39 g). The mixture was stirred for 1 h and transferred to a glass lined 150 ml Parr autoclave vessel where it was reacted for 24 h at 150 °C under constant stirring. The end-point pH of the supernatant was measured.

The solid product was filtered and washed thoroughly with ethanol to remove any organic material not intercalated. Within organo-LDHs, the interlayer water concentration can have a large affect on the arrangement of the organic anions co-habiting the interlayer. To ensure reproducibility and comparability all samples were dried at 80 °C for 24 h and then left to re-hydrate in air for 24 h at room temperature. MgAl(TA) LDHs were synthesised with *R* values of (2.0), (3.0), (4.0), and (5.0) using the method outlined above, where *R* indicates the initial reactant Mg/Al ratio.

Powder X-ray diffraction (PXRD) was carried out on the samples equilibrated with atmospheric humidity using a Philips X'pert PW3710 diffractometer with Cu-Kα radiation (λ = 1.5418 Å). Patterns were obtained using a 2θ range of 2.00 to 80.00 degrees in 0.02 degree increments, each held for 20 s. Fourier transform infra-red (FTIR) spectroscopy was carried out on a ThermoNicolet Nexus spectrometer using a Smart Golden Gate Single Reflection stage Attenuated Total Reflection (ATR), with data recorded as an average of 64 scans between 400 cm^{-1} and 4000 cm^{-1}. CHN elemental analysis was recorded on an Analytical Inc. CE440 instrument. Bulk Mg/Al ratios were determined using ion beam analysis.[49] 5 microCoulombs of 2.50 MeV $^4He^+$ ions were delivered to each sample surface at normal incidence. Backscattered $^4He^+$ ions were detected at 170° to the incident beam with a 1.5 mm thick PIPS detector, having energy resolution of 17 keV. Data were fitted using SIMNRA version 5.0 using Rutherford scattering cross sections for Mg and Al and a non-Rutherford scattering correction for O and C. The thermogravimetric analysis (TGA) was performed on a Polymer Laboratories TGA 1500 instrument. The samples were heated from room temperature to 1200 °C at a ramp rate of 30 °C min^{-1} under a nitrogen atmosphere.

For high-resolution image analysis Field Emission Gun (FEG) SEM was used. The FEG-SEM was carried out on a JEOL 6340F instrument at the Department of Materials Science and Metallurgy, University of Cambridge.

3. Results

Powder X-ray diffraction

The PXRD patterns were indexed on the basis of a rhombohedral lattice within a hexagonal unit cell. The *a* and *c* parameters obtained are outlined in Table 1. It was possible to refine and index the observed powder XRD patterns using the DICVOL91 automatic indexing programme[36] with the exception of the *R*(3.0) pattern. The patterns obtained are illustrated in Fig. 2. Expansions of the regions 2° to 30° and 57° to 65° 2θ are illustrated in Fig. 3 and Fig. 4 respectively. The 10*l* peaks were also indexed using the DICVOL91 algorithm, with all values of *R* showing strong reflections for *hkl* 102 and 108. The indexed 10*l* peaks are summarised in Table 2.

Table 1 Cell parameters for MgAl(TA) LDHs

R	*a*/Å	Mg/Al	*c*/Å[a]	Gallery height/Å
2	3.038(11)	1.8	42.83(13)	9.48
3	3.041/3.087	2.0/6.09	67.34[b]	—
4	3.085(6)	5.8	24.77(7)	3.45
5	3.085(11)	5.7	24.76(13)	3.46

[a] Samples equilibrated with atmosphere. [b] Interstratified phase: based on a 3-layer repeat of 22.4 Å (see Section 4)

Table 2 Observed *hkl* 10l peaks for MgAl(TA) LDHs

	Observed 2θ			
h k l	*R*(2.0)	*R*(3.0)	*R*(4.0)	*R*(5.0)
1 0 2	34.359	—	34.324	34.331
1 0 5	35.675	—	—	—
1 0 8	38.073	—	44.766	44.783
1 0 11	41.391	—	53.152	53.131
1 0 14	45.458	—	—	—
1 0 17	50.086	—	—	—
1 0 20	55.264	—	—	—

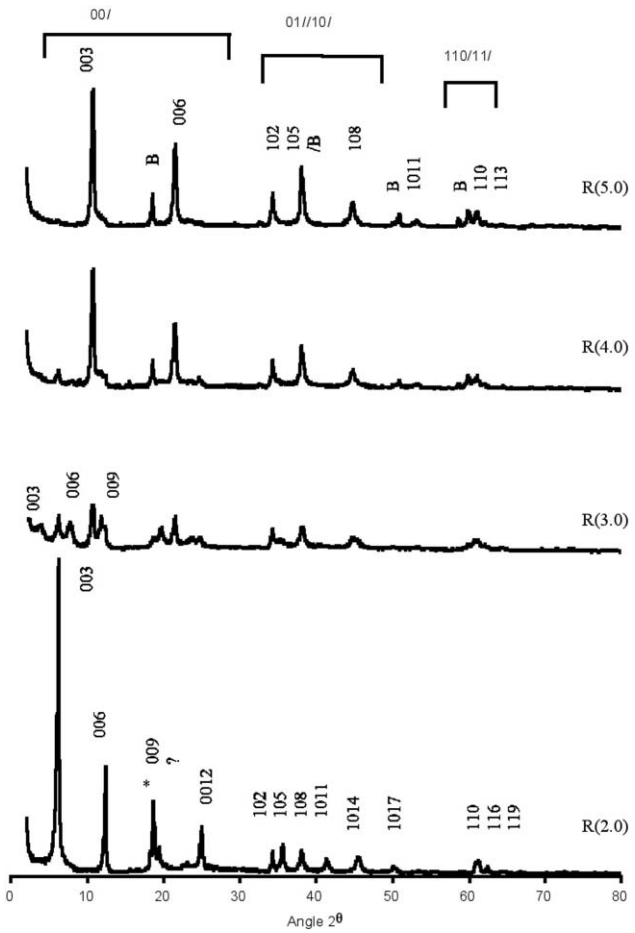

Fig. 2 Powder XRD patterns of MgAl(TA) LDHs formed where B = Brucite, * = gibbsite ($Al(OH)_3$) and ? = possible superlattice reflection.

Fourier transform infra red (FTIR) spectroscopy

The FTIR spectra are also in agreement with those obtained by Newman,[17] who prepared a range of MgAl(TA) LDHs by co-precipitating the metal nitrate salts into a basic solution of the TA and then extensively washing the product to remove excess nitrate. The FTIR spectra for the *R*(2.0), *R*(3.0) and *R*(5.0) MgAl(TA) LDHs is given in Fig. S1 (see ESI†).

Thermogravimetric analysis and elemental analysis

The observed compositions from the elemental analysis of the MgAl(TA) LDHs synthesised are given in Table 3. Water content was obtained from the thermogravimetric analysis

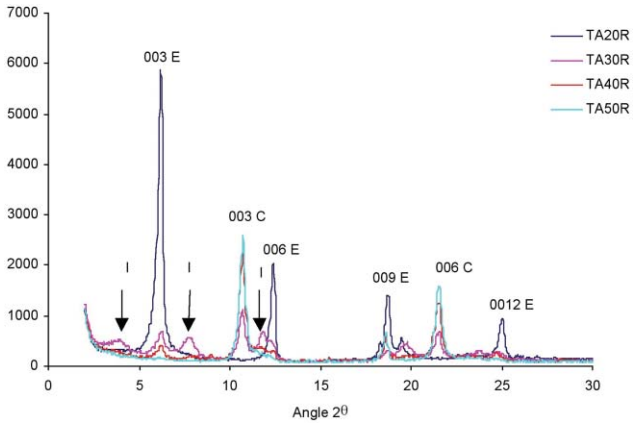

Fig. 3 Powder XRD patterns of MgAl(TA) LDHs in the range 2 to 30° 2θ where I = Interstratified, C = Collapsed and E = Expanded. *Y*-axes shows relative intensity (arbitrary units).

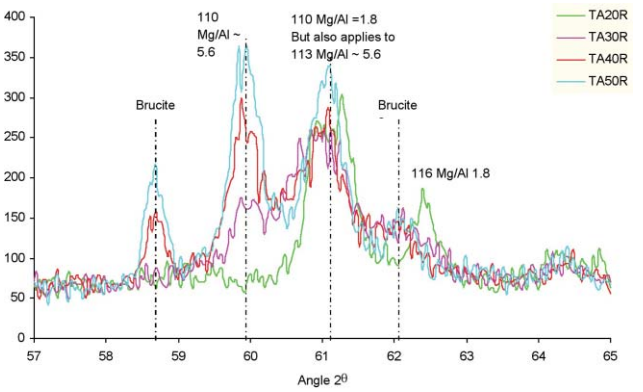

Fig. 4 Powder XRD patterns of MgAl(TA) LDHs in the range 57 to 65° 2θ. *Y*-axes shows relative intensity (arbitrary units).

(TGA) profiles based on the weight loss up to 250 °C (Fig. 5). The purest phase sample by PXRD is that of the *R*(2.0) sample, though a small amount of gibbsite ($Al(OH)_3$) is present within the material. The *R*(3.0) sample contains two phases of different Mg/Al ratio, whilst the *R*(4.0) and *R*(5.0) phases contain brucite. Ion beam analysis was carried out to determine the Mg/Al ratio, giving reasonable agreement with the starting Mg/Al ratios (*R* values) for the *R*(5.0) sample. The data for the *R*(3.0) and *R*(4.0) samples show lower Mg/Al ratios than expected, suggesting that some Mg has been lost on washing. For the *R*(2.0) sample, a Mg/Al of 1.9 was recorded, giving very good agreement with the XRD data (Table 1), indicating that the *R*(2.0) sample contained only minor impurities. As interpretation of elemental analysis data from multi-phase samples (by XRD) is not feasible,

Table 3 The observed composition of the MgAl(TA) LDHs

R	Mg/Al[a]	%C	%H	%N	$\%H_2O$
2.0	1.9	14.29	4.06	0.00	11.4
3.0	2.3	12.51	3.71	0.00	12.3
4.0	2.7	10.76	3.52	0.00	10.0
5.0	4.7	9.15	3.46	0.00	8.4

[a] Mg/Al as determined by ion beam analysis.

Table 4 The observed composition of the *R*(5.0) MgAl(TA) LDH before and after TGA analysis up to 1200 °C

R	%C	%H	%N	H_2O
5.0 pre-TGA	9.15	3.46	0.00	8.4
5.0 post-TGA	0.72	0.65	0.00	—

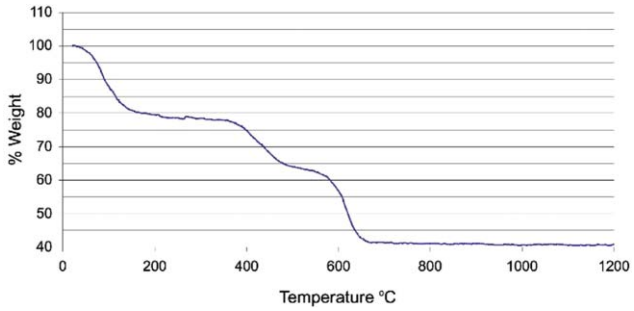

Fig. 5 TGA profile for MgAl (TA) *R*(2.0).

and Mg/Al ratios inconclusive, then only the *R*(2.0) sample is considered. Elemental analysis was also carried out on the residue from the *R*(5.0) sample after TGA. The results prior to, and after, heating to 1200 °C are presented in Table 4.

Scanning electron microscopy

The electron micrographs of the MgAl(TA) LDHs synthesised with ratios *R*(2.0) and *R*(5.0) are given in Fig. 6(a) and 6(b) respectively. Unusually for organo-LDHs, the samples are not of the expected the form where the LDH sheets exhibit wave-like undulations. The samples prepared can be seen to be of hexagonal form, typical of an LDH and compare well with those recently reported by Ogawa and Sugiyama for a highly crystalline ZnAl organo-LDH based on co-hydration of the zinc oxide and aluminium hydroxide precursors.[34]

Crystal size is generally in the range of 1 micron or less. A range of MgAl(TA) LDHs with similar *R*-values are given in Fig. 6(c) to 6(h). In Fig. 6(c) the R2 sample and (d) the R5 prepared by the direct synthesis co-precipitation method are shown (see ESI†); (e) the R2 sample and (f) the R5 prepared by a sol–gel method (see ESI†);[37] and in (g) the R2 sample and (h) the R5 prepared by an urea hydrolysis method (see ESI†).[38] Though, in some cases, the size of any intact hexagonal crystals appears larger, the synthetic method detailed in this paper appears to give crystals with a smaller particle size distribution and fewer surface defects.

For the terephthalate LDH samples prepared using "traditional" methods, the SEM data show a less regular morphology for the direct synthesis co-precipitated samples (Fig. 6(c) and (d)) with some larger particles a few microns across along with some much smaller particles (*ca.* 200 nm or less) on the surface. For the sol–gel and urea methods, the samples were prepared by initial LDH synthesis followed by calcination and rehydration (reconstruction method) and here there is more evidence of the hexagonal platelet LDH morphology. However, there is considerable evidence of surface defects on the particles which is consistent with that observed previously in

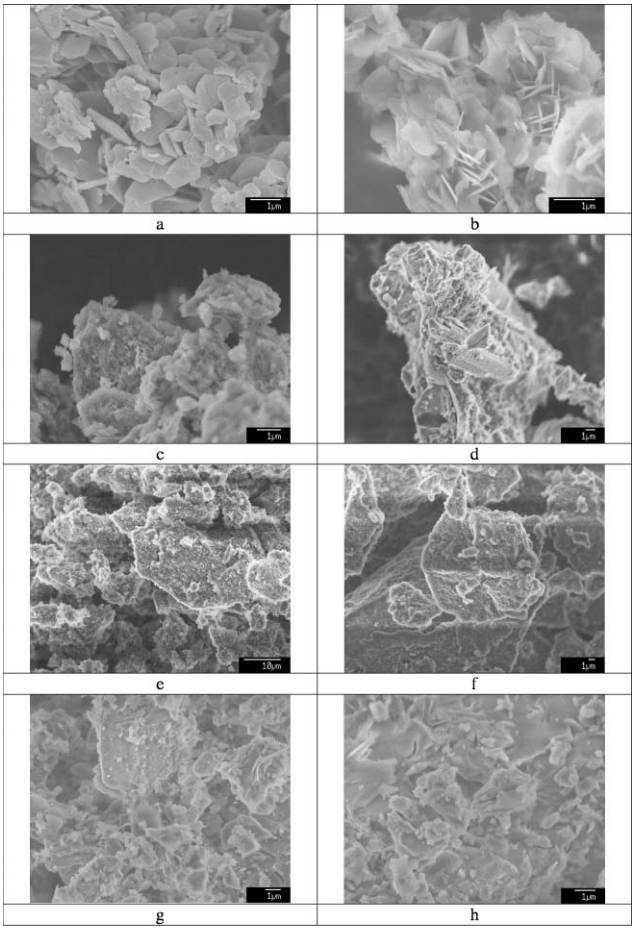

Fig. 6 Scanning electron micrographs of (a) the R2 sample and (b) the *R*(5.0) prepared from the metal hydroxides; (c) the R2 sample and (d) the R5 prepared by the direct synthesis co-precipitation method (see ESI S1†); (e) the R2 sample and (f) the R5 prepared by a sol–gel method (see ESI Fig. S2†); (g) the R2 sample and (h) the R5 prepared by an urea hydrolysis method (see ESI S3†). The lack of surface defects and high degree of structural integrity in the samples prepared by the method described here are apparent.

rehydrated samples,[39] and is in line with the reduced crystallinity of these samples compared with the method described in this paper.

4. Discussion

The PXRD patterns obtained compare well with those of other studies.[24] The expanded structure, *vide infra*, is the predominant phase at *R*(2.0), whilst at *R*(4.0) and *R*(5.0) the collapsed phase dominates. The interstratified phase is found at *R*(3.0), with alternating layers of collapsed and expanded phases. This is more clearly visible in Fig. 3, which shows an expansion of the region 2 to 30 2θ. Brucite is present as an impurity as indicated by the reflection at about 19 and 57 2θ for the *R*(4.0) and *R*(5.0) LDHs. Analysis of the 110 reflections detailed in Fig. 4, using the method of Kaneyoshi and Jones,[40] show that the *R*(2.0) LDH has a Mg/Al ratio of 1.8, whilst the *R*(4.0) and *R*(5.0) LDHs have a Mg/Al of 5.8/5.7. Intercalation of TA is further

confirmed by the FTIR spectra (Fig. S1, see discussion in ESI†). The spectra compare favourably with those obtained for TA in MgGa LDHs.[28]

Control of product Mg/Al ratio

In previous preparations using co-precipitation and anion exchange, it was possible to control to a certain degree the Mg/Al ratio in the product. A slight decrease in the Mg/Al ratio in the product, relative to the starting Mg/Al ratio (*R*), is generally observed.[17] A different situation arises here, where a continuous increase in the product Mg/Al ratio with increasing *R* is not observed. Rather, for the *R*(2.0) LDH a Mg/Al ratio of 1.8 is observed, whilst for *R*(4.0) and *R*(5.0) the LDHs have a Mg/Al ratio of 5.8/5.7. For the *R*(4.0) and *R*(5.0) LDHs an increase in Mg/Al ratio in the product up to 5.6 is noted rather than the decrease as observed with other methods. A similar loss of control of Mg/Al ratio is also encountered when using metal oxides as precursors, suggesting that the co-hydration of the metal oxides and the mechanism here may be similar.[30]

The formation of a higher Mg/Al ratio in the product than present in the initial solution has previously been reported and is explained by the formation of AlOOH, which has its most intense reflection (020) at around 14.5 2θ.[41,42] However, this reflection is absent in the *R*(5.0) pattern, and very weak in the *R*(4.0) pattern, obtained by this method. The $Al(OH)_3$ reflection at 18.3 2θ is absent in both cases. In addition to this brucite is present in both *R*(4.0) and *R*(5.0), with the greater amount being present in the *R*(4.0) product. This would suggest that even more AlOOH should be formed to attain a Mg/Al ratio of 5.6. An explanation for the Mg/Al ratio of 5.6 is that the excess Al exists in a poorly crystalline or amorphous phase.

It is noted that, in the *R*(2.0) sample, $Al(OH)_3$ is present as a minor impurity (18.3° 2θ), and a reflection at 19.5° 2θ is indicative of a possible super-lattice. This has previously been reported for terephthalate intercalated LDHs.[41] This super-lattice seems only to form during hydrothermal treatment of the samples. As Mg^{2+} and Al^{3+} have very similar scattering factors for X-rays, it seems that this super-lattice reflection must suggest increased order within the interlayer anions. The disappearance of this reflection in the collapsed phase also supports this view, although it is interesting to note that there is an intense reflection at this value in the interstratified sample, though this is also in the region of the 0015 reflection. The 0012 reflection is consistently absent from the interstratified phase. The presence of a super-lattice in the interstratified sample suggests that those TA anions within expanded phases retain a high degree of order.

Mechanism of formation

In these syntheses, the pH of the solution was not controlled but varied around an initial pH 9.5, with a slight decrease in the pH of the product supernatant. The affect of pH on product formation has previously been investigated by others, extracting aliquots from the variable pH co-precipitation reaction mixture over time,[28] or by systematically varying the pH during constant pH co-precipitation reactions.[27] In both cases, lower pH resulted in a higher TA content, presumably due to less carbonate being present, but with a loss of control of the product Mg/Al ratio towards low values relative to the starting solution.[28] Conversely, a high pH of 10 or greater resulted in good control of the Mg/Al ratio, but poor control of the TA anion uptake. The loss of control of the Mg/Al ratio at lower pH is probably linked to the solubility of the M^{2+}/M^{3+} species. Interestingly Weir *et al.* obtained the sharpest reflections, indicating greater crystalline nature, for Mg–Ga-TA and Mg–Al-TA at pH 7.7, suggesting that the terephthalic acid may not be fully dissociated.[28] At this pH for *R*(2.0) to *R*(4.0) LDHs all the products were observed to be the expanded phase with Mg/Al ratios of less than 2.

In our work, using the hydrothermal method of synthesis, pH has been high at around pH 9.5, but the PXRD analysis shows that the cation ratio has not been controlled, and does not necessarily follow the initial reactant Mg/Al ratio. Previous studies have utilised the nitrate salts of Mg and Al as source materials whilst in this current work the hydroxides have been used. It is possible that the method of synthesis is critical with the co-precipitation method involving drop-wise addition of the two dissolved metal salts, whilst here the essentially insoluble salts are combined prior to hydrothermal treatment. By definition, co-precipitation involves one metal salt precipitating at a given pH and this process causing other metal salts to co-precipitate at a pH at which this would not otherwise occur. To achieve this, the nucleation and precipitation processes must occur from solution to the solid phase and must be extremely rapid which generally leads to smaller and less crystalline particles.[43] Subsequent ageing in the mother liquor and/or by hydrothermal treatment can enhance crystallinity and lead to larger crystals by Ostwald ripening. By comparison, the method described here involves solid precursors (metal hydroxides) undergoing a process driven by Ostwald ripening (*i.e.* dissolution of some sparingly soluble material followed by re-precipitation onto an existing crystal surface). This process takes place more slowly and presumably through an epitaxial type of growth leading to the more crystalline products we observe.

Interestingly in our results using the hydrothermal preparation, sharp peaks are found in the 01*l*/10*l* region, rather than the typical "saw-tooth" pattern indicative of turbostratic disorder. The presence of high orders of reflections in this region suggests a highly ordered interlayer TA anion arrangement, which is in agreement with the emergence of a 100 reflection indicating super-lattice formation, though in previous studies a 100 reflection is observed alongside broad higher order (0114 and above) reflections.[41]

Interlayer arrangement and interstratification

Owing to the relatively rigid nature of the TA anion, the number of possible conformations that it can adopt within the interlayer is limited. So far three distinct arrangements have been postulated—collapsed, interstratified, and expanded (see Fig. S2 in ESI†). The expanded phase corresponds to an interlayer spacing of approximately 14 Å. Allowing for a layer thickness of 4.8 Å this leaves a gallery height of 9.2 Å, corresponding to the length of a TA anion along its longest axis (*ca.* 9.5 Å). Therefore the TA anions are arranged with their long axis perpendicular to the hydroxyl layers as shown in Fig. S2(a), ESI†. The collapsed phase is the phase where it is believed that the TA anion is oriented with its long axis and molecular plane lying parallel to the layers. This orientation results in an interlayer spacing of

circa 8.1 Å, and a gallery height of around 3.3 Å (Fig. S2(b), ESI†). The interstratified phase is illustrated in Fig. S2(c), ESI†. It is a regular repeat of one collapsed (8 Å) and one expanded (14 Å) interlayer arrangement and is recognised by an interlayer spacing in the region of 22 Å. The arrangement of the TA anion in this phase was first reported by Vucelic *et al.* in a MgAl LDH at 75 °C.[41]

The factors that govern the interlayer arrangement are complex and not fully understood. The vertical arrangement of TA within the gallery region was first observed by Drezdon who prepared Mg–Al(TA) LDHs with *R*(2.0).[11] A similar result was subsequently reported by others within a variety of LDHs of *R*(2.0) and *R*(3.0).[20,21,24] Thermal studies of Mg–Al(TA) LDHs with *R*(2.0) showed that a non-hydrothermally treated sample maintained the expanded phase up to 250 °C whereas a hydrothermally treated sample underwent an abrupt transformation to give an increased basal spacing of around 22 Å at 75 °C.[35] Further heating to 250 °C resulted in a drop in interlayer spacing to approximately 8 Å, *i.e.* a collapsed structure. Further work by Kooli and co-workers showed that layer charge, that is M^{2+}/M^{3+} ratio, also controlled the nature of the anion arrangement, with MgAl(TA) LDHs of *R*(1.0) and (2.0) resulting in an expanded phase whilst *R*(3.0) and (4.0) gave the collapsed phase.[25]

The influence of pH during preparation on the phase obtained has been analysed, showing that at about pH 8.5 and below the expanded phase is the only one formed even at *R*(4.0).[16,27,28] This observation has been explained by the influence of pH on impurity anion content as carbonate content increases substantially above pH 8.5.[16,27] Interestingly these previous studies show that intercalated TA concentrations increase as pH drops with highest values reported at pH 6.5, acidic conditions, suggesting that in this case the TA may not be fully dissociated. These observations may be rationalised in that, at high pH, the TA anion is more soluble and is less likely to be intercalated. At low pH the protonated acid is hydrophobic and has affinity for the gallery region. Alternatively, the basic nature of the interlayer region may result in the *in situ* deprotonation of the terephthalic acid as has been suggested for anion incorporation in charge neutral layered materials.[44]

Newman *et al.* investigated the effect of hydration state on the TA interlayer arrangement, finding that both layer charge and degree of hydration affected the product TA arrangement.[9,17] The authors made extensive use of molecular dynamics computer simulation to reinforce experimental evidence. Other work[28] suggested that the interstratified phase could be due to two different interlayer species, TA layers of 14.2 Å and CO_3^{2-} layers of 7.6 Å, as observed in the carbonate/sulfate system.[45] However, subsequent work showed that the interstratified form arises from the dehydration of samples where all the layers are initially expanded, and thus the collapsed layers in the interstratified phase must contain TA.[9,17,46,47] Recently, Greenwell and Coveney suggested that the interstratified arrangement may be due to asymmetric distribution of TA anions in adjacent interlayers, with a high degree of replication resulting.[48]

In our work, from the 11*l* region of the PXRD pattern (Fig. 4), it initially appears that the *R*(3.0) interstratified LDH has a Mg/Al 6.09 phase present as indicated by the 110 reflection at 59.9 2θ and the 113 reflection found at 61.1 2θ. However, the 110 reflection is very weak in comparison to the 113 reflection, when compared to the intensity distribution observed for the *R*(4.0) and *R*(5.0) LDHs. If the *R*(2.0) LDH is considered, it can be seen that the *R*(2.0) 110 reflection overlaps with the *R*(4.0)/(5.0) 113 reflection. Therefore we conclude the *R*(3.0) LDH product contains a mixture of two phases, one with a Mg/Al ratio of 6.09, the other with a Mg/Al ratio of 2.0. The formation of the interstratified phase is of interest as the Mg/Al ratio, and presumably TA/water content, of the two phases present in the *R*(3.0) PXRD pattern are not dissimilar those within the *R*(2.0) and *R*(5.0) products, neither of which show interstratification suggesting a possible third phase.

Table 5 Calculated anion dependence of LDH composition

Formula	%C	%H
Observed sample Mg/Al 1.8 11.4% H_2O	14.29	4.06
$[Mg_{1.8}Al(OH)_{5.6}]TA_{0.5}1.77H_2O$	17.16	4.01
$[Mg_{1.8}Al(OH)_{5.6}]CO_{3\,0.12}TA_{0.38}1.68H_2O$	14.28	3.98
$[Mg_{1.8}Al(OH)_{5.6}]HCO_{3\,0.24}TA_{0.38}1.74H_2O$	14.36	3.98
$[Mg_{1.8}Al(OH)_{5.6}]OH_{0.22}TA_{0.39}1.67H_2O$	14.20	4.09

Interlayer composition and hydration state

The effect of any impurity anions on the observed elemental composition of the *R*(2.0) LDH for given water content is investigated in Table 5. In general for preparation of LDHs at high pH, CO_3^{2-} predominates due to the high solubility of atmospheric CO_2, whilst as the pH is decreased HCO_3^- becomes more prevalent. In addition, at low pH the counter anion in the metal salt, in this case OH^-, will be present in solution at greater concentration.

The ideal formula (see Table 5) with no impurity anions is inaccurate with respect to %C indicating that there are other species present within the interlayer. The influence of various other charge balancing anions upon the elemental composition at the observed Al content was calculated. The water content was kept constant at the observed percentage mass value, whilst the stoichiometric TA anion content was varied in 0.01 increments. The formulae that best fitted the observed elemental composition are reported in Table 5. It is interesting to note that no matter which impurity anion is chosen, the best-fit formulae obtained are near identical with respect to TA content. To ascertain whether this result is general, the same calculation was applied to the results obtained by Newman for a Mg–Al(TA) LDH of Mg/Al ratio 1.8 synthesised by constant pH co-precipitation.[17] The observed and calculated compositions are reported in Table 6. It can be seen that a similar result is obtained. Further, allowing for the different degree of

Table 6 Anion dependence of LDH composition reported by Newman[12]

Formula	%C	%H
Observed Mg/Al 1.8, 18.5% H_2O	13.40	4.60
$[Mg_{1.8}Al(OH)_{5.6}]TA_{0.5}\cdot3.13H_2O$	15.79	4.59
$[Mg_{1.8}Al(OH)_{5.6}]CO_{3\,0.11}TA_{0.39}\cdot2.98H_2O$	13.36	4.56
$[Mg_{1.8}Al(OH)_{5.6}]HCO_{3\,0.22}TA_{0.39}3.07H_2O$	13.43	4.56
$[Mg_{1.8}Al(OH)_{5.6}]OH_{0.20}TA_{0.40}\cdot2.96H_2O$	13.33	4.66

hydration, both sets of calculations agree closely on the number of TA anions incorporated. This result does not, of course, preclude the possibility of more than one impurity species being present.

It is interesting to note that despite having the same Mg/Al ratio, similar TA anion content, and both samples being dried and re-hydrated, the water content is considerably different. This could be due to the surface area and pore size distribution of the samples (not analysed in the present study), as it might be expected that the amount of pore space in the sample will vary according to crystal size. Studies have shown that both allowing the pH to vary and hydrothermal treatment can affect the average pore diameter and specific surface area of the product obtained.[26] Elemental analysis carried out on the *R*(5.0) LDH sample after heating to 1200 °C for thermogravimetric analysis showed that there were carbon and hydrogen containing residues left within the material (Table 4).

The degree of TA intercalation using the hydrothermal synthesis, based on the above results, is between 76% and 80% of the anion exchange capacity. This is despite the fact that in this preparation only a stoichiometric amount of TA to Al^{3+} was used, whilst Newman used a 20-fold excess, indicating the attractiveness of the hydrothermal route for green chemistry preparation of organo-LDHs.[17] Kukkadapu *et al.* quote a molar content in excess of 95% at pH 7.5 and below, however the products were only washed with water so assuming that the TA is not dissociated and thus insoluble at this pH it is possible that their product contains un-dissociated TA.[27]

5. Conclusions

MgAl-organo LDHs have been prepared intercalated with terephthalate anions, by an environmentally attractive method using stoichiometric amounts of terephthalate, and from the metal hydroxides. The reaction was found to be highly efficient with a high degree of uptake of terephthalate observed despite there being only a slight excess of the anion in the reaction. Similar results were obtained to the conventional co-precipitation method where up to 20-fold excess of the terephthalate is required, and large quantities of highly basic waste solution are produced. The efficiency of organic anion incorporation and lack of competing counter ions, *e.g.* nitrate or chloride, suggest that the hydrothermal preparation route could be used for the preparation of LDHs intercalated with pharmaceutically active compounds for slow release drug delivery. The samples were found to be highly ordered, especially at a Mg/Al ratio of 2.0. SEM analysis showed very clean crystals with narrow particle size distribution, few surface defects and with high aspect ratios, relative to other methods of synthesis.

Acknowledgements

The authors would like to thank the Microanalysis Section, Department of Chemistry, University of Cambridge for carrying out CHN elemental analysis, Dr David Vowles, Department of Materials Science and Metallurgy, University of Cambridge for carrying out SEM.

References

1 K. H. Goh, T. T. Lim and Z. L. Dong, *Environ. Sci. Technol.*, 2009, **43**, 2537–2543.
2 N. Barakos, S. Pasias and N. Papayannakos, *Bioresour. Technol.*, 2008, **99**, 5037–5042.
3 L. Latterini, M. Nocchetti, G. G. Aloisi, U. Constantino, F. C. De Schryver and F. Elisei, *Langmuir*, 2007, **23**, 12337–12343.
4 M. Wei, M. Pu, J. Guo, J. B. Han, F. Li, J. He, D. G. Evans and X. Duan, *Chem. Mater.*, 2008, **20**, 5169–5180.
5 Y. N. Chan, T. Y. Juang, Y. L. Liao, S. A. Dai and J. J. Lin, *Polymer*, 2008, **49**, 4796–4801.
6 D. G. Evans and R. C. T. Slade, *Struct. Bonding*, 2006, **119**, 1–87.
7 F. O. Figueras, *Top. Catal.*, 2004, **29**, 189–196.
8 T. Hibino and M. Kobayashi, *J. Mater. Chem.*, 2005, **15**, 653–656.
9 A. S. Bookin and V. A. Drits, *Clays Clay Miner.*, 1993, **41**, 551–557.
10 E. Géraud, S. Rafqah, M. Sarakha, C. Forano, V. Prevot and F. Leroux, *Chem. Mater.*, 2008, **20**, 1116–1125.
11 M. A. Drezdzon, *Inorg. Chem.*, 1988, **27**, 4628–4632.
12 H. Kominami, S. Kurimoto, M. Kubota, R. Shiozaki and Y. Kera, *J. Ceram. Soc. Jpn.*, 1997, **105**, 707–709.
13 J. Evans, M. Pillinger and J. J. Zhang, *J. Chem. Soc., Dalton Trans.*, 1996, 2963–2974.
14 M. A. Ulibarri, F. M. Labajos, V. Rives, W. Kagunya, W. Jones and R. Trujillano, *Mol. Cryst. Liq. Cryst.*, 1994, **244**, 167–172.
15 T. Challier and R. C. T. Slade, *J. Mater. Chem.*, 1994, **4**, 367–371.
16 R. S. Maxwell, R. K. Kukkadapu, J. E. Amonette and H. Cho, *J. Phys. Chem. B*, 1999, **103**, 5197–5203.
17 S. P. Newman, Structural Studies of Layered Anion Exchangers: Simulation and Measurement. *PhD Thesis*, University of Cambridge, 1999.
18 S. P. Newman and W. Jones, *J. Solid State Chem.*, 1999, **148**, 26–40.
19 Z. L. Huang, M. Drillon, N. Masciocchi, A. Sironi, J. T. Zhao, P. Rabu and P. Panissod, *Chem. Mater.*, 2000, **12**, 2805–2812.
20 M. Meyn, K. Beneke and G. Lagaly, *Inorg. Chem.*, 1990, **29**, 5201–5207.
21 F. Kooli, V. Rives and M. A. Ulibarri, *Mater. Sci. Forum*, 1994, **152–153**, 375–346.
22 W. T. Reichle, *Solid State Ionics*, 1986, **22**, 135–141.
23 M. A. Ulibarri, F. M. Labajos, V. Rives, R. Trujillano, W. Kagunya and W. Jones, *Inorg. Chem.*, 1994, **33**, 2592–2599.
24 W. Kagunya, M. Chibwe and W. Jones, *Mol. Cryst. Liq. Cryst.*, 1994, **244**, 155–160.
25 F. Kooli, I. C. Chisem, M. Vucelic and W. Jones, *Chem.Mater.*, 1996, **8**, 1969–1977.
26 E. L. Crepaldi, P. C. Pavan and J. B. Valim, *J. Braz. Chem. Soc.*, 2000, **11**, 64–70.
27 R. K. Kukkadapu, M. S. Witkowski and J. E. Amonette, *Chem. Mater.*, 1997, **9**, 417–419.
28 M. R. Weir, J. Moore and R. A. Kydd, *Chem. Mater.*, 1997, **9**, 1686–1690.
29 H. C. Greenwell, W. Jones, D. N. Stamires, M. F. Brady and P. O'Connor, *Green Chem.*, 2006, **8**, 1067–1072.
30 H. C. Greenwell, C. C. Marsden and W. Jones, *Green Chem.*, 2007, **9**, 1299–1307.
31 Z. P. Xu and G. Q. Lu, *Chem. Mater.*, 2005, **17**, 1055–1062.
32 S. Mitchell, T. Biswick, W. Jones, G. Williams and D. O'Hare, *Green Chem.*, 2007, **9**, 373–378.
33 S. Mitchell, I. R. Baxendale and W. Jones, *Green Chem.*, 2008, **10**, 629–634.
34 M. Ogawa and Y. Sugiyama, *J. Ceram. Soc. Jpn.*, 2009, **117**, 179–184.
35 M. Ogawa and S. Asai, *Chem. Mater.*, 2000, **12**, 3253–3255.
36 A. Boultif and D. Louer, *J. Appl. Crystallogr.*, 1991, **24**, 987–993.
37 T. López, P. Bosch, E. Ramos, R. Gómez, O. Novaro, D. Acosta and F. Figueras, *Langmuir*, 1996, **12**, 189–192.
38 U. Costantino, F. Marmottini, M. Nocchetti and R. Vivani, *Eur. J. Inorg. Chem.*, 1998, (10), 1439–1446.
39 H. C. Greenwell, P. J. Holliman, W. Jones and B. Vaca Velasco, *Catal. Today*, 2006, **114**, 397–402.
40 M. Kaneyoshi and W. Jones, *J. Mater. Chem.*, 1999, **9**, 805–811.
41 M. Vucelic, G. D. Moggridge and W. Jones, *J. Phys. Chem.*, 1995, **99**, 8328–8337.

42 M. Vucelic, W. Jones and G. D. Moggridge, *Clays Clay Miner.*, 1997, **45**, 803–813.
43 H. C. Greenwell, L. A. Bindley, P. R. Unwin, P. J. Holliman, W. Jones, P. V. Coveney and S. L. Barnes, *J. Cryst. Growth*, 2006, **294**, 53–59.
44 P. V. Kamath, G. H. A. Therese and J. Gopalakrishnan, *J. Solid State Chem.*, 1997, **128**, 38–41.
45 A. S. Bookin, V. I. Cherkashin and V. A. Drits, *Clays Clay Miner.*, 1993, **41**, 558–564.
46 S. P. Newman, S. J. Williams, P. V. Coveney and W. Jones, *J. Phys. Chem. B*, 1998, **102**, 6710–6719.
47 M. Kaneyoshi and W. Jones, *Chem. Phys. Lett.*, 1998, **296**, 183–187.
48 H. C. Greenwell and P. V. Coveney, *Orig. Life. Evol. Bio.*, 2006, **36**, 13–37.
49 *Handbook of Modern Ion Beam Materials Analysis*, ed. J. R. Tesmer and M. Nastasi, Materials Research Society, Pittsburgh, 1995.